



Cite this: DOI: 10.1039/d5fo04976h

# Modulation and adaptation of gut microbial metabolic functions under probiotic and postbiotic treatment using a novel *in vitro* anaerobic pseudo-colon system

Nehal Batra,<sup>a</sup> Prangya Ranjan Rout<sup>b</sup> and Priyankar Dey \*<sup>a</sup>

Probiotic and postbiotic compounds found in food influence gut microbiota to attenuate chronic metabolic diseases; however, the underlying mechanisms are not yet fully understood. This study employed a customized *in vitro* anaerobic pseudo-colon system (AMMR) to evaluate the impacts of *Lactiplantibacillus plantarum* (probiotic) and butyrate (postbiotic) on gut microbial composition and functionality, using human fecal samples. Metagenomic (16S rRNA) profiling and untargeted metabolomic (GC-MS) analysis were conducted after 48 h treatments. The results showed that butyrate supplementation markedly enhanced microbial diversity, inhibited opportunistic pathobionts (e.g., *Enterococcus* and *Klebsiella*), and selectively enriched butyrate producers (e.g., *Lachnoclostridium*), while diminishing the Firmicutes : Bacteroidetes ratio. It increased indole levels metabolically and redirected pathways towards amino acid synthesis and energy metabolism, while suppressing fatty acid formation. In contrast, *L. plantarum* exhibited modest alterations in microbial diversity while enhancing *Bacteroides* and *Klebsiella* and preserving elevated *Enterococcus* levels. It elevated saturated fatty acids (octanoic/capric acid) and enhanced amino acid catabolic pathways (valine/leucine) and redox regulators (taurine metabolism). Correlation analysis revealed that butyrate was associated with fiber-degrading microbes, whereas *L. plantarum* was associated with lactic acid bacteria, suggesting distinct ecological niches and interaction patterns. These findings collectively indicate that butyrate and *L. plantarum* elicit complementary microbial alterations, i.e., butyrate directly transforms the microbial structure and metabolism towards an anti-inflammatory phenotype, while *L. plantarum* largely influences *via* metabolic byproducts and niche adjustment. The complementary actions highlight the therapeutic potential of integrated probiotic–postbiotic approaches for the enhancement of gut health.

Received 17th November 2025,  
Accepted 27th February 2026

DOI: 10.1039/d5fo04976h

[rsc.li/food-function](https://rsc.li/food-function)

## Introduction

Emerging gut microbiota-centric approaches, comprising probiotics (beneficial live microorganisms), prebiotics (microbe-feeding), postbiotics (microbe-derived metabolites), and synbiotics (synergistic combinations), are transforming translational research by facilitating a favourable modulation of the host–microbiome axis to prevent or address metabolic, immune, and neuropsychiatric disorders. By defining mechanistic pathways, such as the improvement of gut barrier integrity, modulation of systemic inflammation, and production of bioactive compounds, these interventions expedite the trans-

lation of microbiome research into targeted therapeutics and personalized nutrition strategies.<sup>1</sup>

*Lactiplantibacillus plantarum* is one of the most extensively studied probiotics, which can mitigate irritable bowel syndrome, diminish pathogenic bacterial burdens, and enhance the prevalence of gut commensals (e.g., *Bifidobacterium*) and butyrogenic bacteria in clinical settings.<sup>2</sup> Comparable to other probiotic bacteria, lactate produced by *L. plantarum* can be employed by cross-feeding microorganisms to produce butyrate,<sup>3</sup> so indirectly affecting the gut metabolome. Nevertheless, the probiotic efficacy may be limited by the survival of viable cells during gastrointestinal transit, with viability reductions undermining therapeutic results. Short-chain fatty acids (SCFAs), especially butyrate, are a multifunctional postbiotic, produced during bacterial fermentation of dietary fibers. Butyrate functions as the primary energy source for colonocytes, improves mucosal barrier integrity by stabilizing hypoxia-inducible factor, and attenuates epithelial per-

<sup>a</sup>Department of Biotechnology, Thapar Institute of Engineering and Technology, Patiala 147004, Punjab, India. E-mail: priyankar.dey@thapar.edu, priyankardey28@gmail.com; Tel: +91-9064275660

<sup>b</sup>Department of Biotechnology, Dr B.R. Ambedkar National Institute of Technology, Jalandhar, India



meability.<sup>4</sup> Its immunomodulatory activities encompass the inhibition of histone deacetylases, modification of regulatory T-cell differentiation, and reduction of pro-inflammatory cytokines.<sup>5</sup> Pre-clinical and clinical studies have shown that butyrate supplementation reduces the severity of colitis, facilitates remission of inflammatory bowel disease (IBD), and safeguards against pathogen-induced mucosal injury.<sup>6</sup>

Probiotics utilize living microorganisms to provide health benefits through direct interactions with the host and the generation of metabolites, whereas postbiotics, such as butyrate, eliminate the necessity for microbial viability, providing benefits in terms of stability, safety, and uniformity. Comparative research indicates that postbiotics may have more significant microbiome modulatory effects in specific situations;<sup>7</sup> nonetheless, comprehensive direct comparisons with probiotics under controlled settings are scarce. Despite comprehensive research on both *L. plantarum* and butyrate, it remains unclear whether the health-promoting effects of probiotic consumption are predominantly attributable to live bacterial activity or metabolites like butyrate. Therefore, we hypothesized that supplementation with *L. plantarum* and butyrate would induce unique but potentially complementary alterations in the gut microbiome composition and metabolite profiles using a novel *in vitro* pseudo-colon system. Specifically, we hypothesized that *L. plantarum* would induce extensive alterations in microbial diversity and competitively exclude opportunistic pathogens *via* live cell interactions and diverse metabolite synthesis. Butyrate supplementation, on the other hand, was expected to augment anti-inflammatory metabolomic signatures without substantially modifying living community composition. This direct comparison was expected to elucidate both overlapping and unique impacts, thereby defining the degree to which butyrate facilitates the probiotic activities of *L. plantarum*. Collectively, this direct comparison elucidates the gut-level mechanisms of probiotic–postbiotic action and guide focused therapy options for gut health management.

## Materials and methods

### Chemicals and reagents

Gifu anaerobic medium and sodium butyrate were purchased from HiMedia, India. Oxgall, sodium hydrogen carbonate, pancreatin, sodium sulphate, and *n*-hexane were acquired from LOBA Chemie, India. *N,O*-Bis(trimethylsilyl)trifluoroacetamide was purchased from Sigma-Aldrich, USA. Sodium hydroxide and hydrochloric acid for pH adjustment were purchased from Rankem, India. Distilled water was obtained using a Millipore Milli-Q ultra-pure water ( $\Omega$ 18.2) system.

### Functioning of the artificial colon model for microbiota research (AMMR)

To replicate the human colonic luminal microenvironment, we have designed and developed a proprietary, fully customizable anaerobic gut microbiome culturing system named the AMMR system (Indian design patent #394577-001; Indian patent appli-

cation #202311013073; PCT #PCT/IN2023/050834). The benefits of the anaerobic *in vitro* gut microbiome culturing system have been recognized<sup>8–11</sup> and applied for the understanding of microbiota and nutrient reciprocal interactions independent of the host influence.<sup>12–14</sup> The AMMR system comprises two stainless-steel modular units, left and right, each with dimensions of 540 mm (*L*) and 215 mm (*H*). Each unit comprises three independent interconnected anaerobic reactors mimicking the ascending, transverse, and descending colon of the human intestine. The internal architecture of each reactor includes a stainless-steel baffle with a bottom opening space for homogeneous mixing of the fecal slurry and mimicking the peristaltic movement of the human gut. The individual reactor vessel has a total volume of 500 mL (400 mL of effective volume and 100 mL of headspace) and contains 5 ports (1/4") each for pH sensing, headspace gas collection, liquid sample collection, gas purge, and feed addition. The reactor lid with several access ports is connected to the vessel using autoclavable gaskets and clamp-based seals, ensuring airtight closure. When not in use, each port is sealed to maintain sterility and anaerobic conditions.

Both left and right units can be controlled by the common central control unit that continuously monitors and regulates the reactor temperature and pH. Temperature control could be achieved in the range of room temperature ( $\sim$ 25 °C) to a maximum of 80 °C using an external water jacket coupled with an integrated thermostat. The system can be used for both batch and fed-batch modes of operation. Each of the six reactors is independently detachable from the adjacent reactors for easy cleaning, sterilization and handling purposes. This configuration allows either for individual operation of isolated reactors (representing a specific region of the intestine) or combined operation of 3 reactors (representing ascending, transverse, and descending colon). A fed-batch and individual operation approach was used for the current study. Adjacent reactors remain connected through sealed connectors, allowing one-way flow of effluent. All the reactor chambers can be independently flushed with N<sub>2</sub> gas to ensure an anaerobic environment for optimal *in vitro* gut microbial growth.

### Sample collection

The following experiments were conducted under established rules and regulations. The approval for the experiment was acquired from the Institutional Ethical Committee (TIET/EC/2023-08). Informed consent was obtained from human participants of this study. The experiment objectives were explained to all 5 donors (SI Table S1) and they signed an informed consent form for fecal matter donation, and a questionnaire regarding age, ethnicity, food type, medical history, *etc.*, was also obtained at the time of sample collection. The donors had not received any antibiotic treatments or probiotic supplements for at least 3 months before donating the fecal sample.<sup>15</sup>

### *L. plantarum* strain acquisition and evaluation of probiotic characteristics

*L. plantarum* MTCC 2621 (equivalent to ATCC 8014; *Lactiplantibacillus plantarum*) was acquired from the Microbial



Type Culture Collection (MTCC), Council of Scientific & Industrial Research – Institute of Microbial Technology (CSIR-IMTech), Chandigarh, India, and was cultured and maintained under standard conditions. These strains were stored as 20% glycerol stock (v/v) under freezing conditions ( $-80\text{ }^{\circ}\text{C}$ ). The glycerol stock was used as the inoculum and was grown in Gifu anaerobic medium, which was then used directly as the inoculum for treatment.

### Experimental design

Pooled fecal samples from  $n = 5$  individuals were used for the preparation of the stock fecal slurry solution.<sup>16–19</sup> In brief, morning fecal sample was collected individually from the donors in sterile containers, pooled and mixed with Gifu anaerobic medium containing  $13.5\text{ g L}^{-1}$  digested serum, liver extract ( $1.2\text{ g L}^{-1}$ ),  $5\text{ g L}^{-1}$  soluble starch, L-cysteine hydrochloride ( $300\text{ mg L}^{-1}$ ), sodium thioglycolate ( $300\text{ mg L}^{-1}$ ), soya peptone ( $3\text{ g L}^{-1}$ ), and HM peptone B ( $2.2\text{ g L}^{-1}$ ).<sup>20–22</sup> Samples were homogenized in the media and directly used for inoculation in the AMMR system through the entry port (Fig. 1). Three independent reaction mixtures were prepared to evaluate the effect of comparative probiotic and postbiotic treatments on gut microbiota in terms of gut microbial population diversity and overall metabolome: control group, butyrate (postbiotic) treated group, and *L. plantarum* (probiotic) treated group ( $n = 3$  sets for each treatment). The chemical composition of each treatment was uniform, i.e., Gifu anaerobic medium (5.9%), oxgall powder (0.6%), sodium hydrogen carbonate (1.25%), and pancreatin (0.1%).<sup>23</sup> The pH of each of the reactors was maintained at 7.5–8.0, which critically maintained the gut microbial populations.<sup>24,25</sup> In *L. plantarum* treatment,  $1 \times 10^6\text{ CFU mL}^{-1}$  was inoculated, and 20 mM butyrate (corresponding to colonic concentration in healthy individuals) was added for butyrate treatment.<sup>26,27</sup> After feeding was done at 0 h, the reactors were flushed with  $\text{N}_2$  gas and allowed to run for 48 h at  $37\text{ }^{\circ}\text{C}$ .<sup>28,29</sup> Feeding of media was done every 4 h to maintain optimal nutrient availability. After completion of the incubation period, samples were collected from

chamber 3 under aseptic conditions for metabolomic and metagenomic analysis.

### Sample preparation for untargeted metabolomics

Gas Chromatography-Mass Spectrometry (GC-MS)-based untargeted metabolomics was performed to elucidate the metabolic profile under each treatment. The culture medium (2 mL) was mixed with 2 mL of *n*-hexane and 100  $\mu\text{L}$  of *N,O*-bis(trimethylsilyl)trifluoroacetamide, vortexed vigorously for 30 min, and incubated at  $40\text{ }^{\circ}\text{C}$  for 4 h at 200 rpm. The mixture was allowed to settle down, the upper organic layer was separated, and centrifuged at 10 000 rpm for 15 min. The supernatant obtained was mixed with a few granules of sodium sulfate, vortexed for 10 min, and centrifuged at 10 000 rpm for 15 min. The resultant mixture was filtered through a  $0.2\text{ }\mu\text{m}$  syringe filter, and finally transferred to autosampler vials and sealed with a polytetrafluoroethylene cap.

### GC-MS analysis

The metabolite extract was analyzed using an SHS-40 instrument (Massachusetts, USA) equipped with a Bruker 436-GC series, SCION-SQ-MS model, and Rxi®-17Sil-ms column ( $30\text{ m} \times 0.25\text{ mm} \times 0.25\text{ }\mu\text{m}$ ). The initial temperature of the program was set at  $60\text{ }^{\circ}\text{C}$  (solvent delay of 5 min) with a hold time of 4 min, followed by a ramp of  $5\text{ }^{\circ}\text{C min}^{-1}$ , and the end temperature was set at  $280\text{ }^{\circ}\text{C}$  with a hold time of 10 min. The derivatized samples (1  $\mu\text{L}$ ) were injected in splitless mode, with a constant drift of helium gas ( $1\text{ mL min}^{-1}$ ). The MS transfer line temperature was kept at  $280\text{ }^{\circ}\text{C}$ . Automated Mass Spectral Deconvolution and Identification System (AMDIS) version 2.70 was used to analyze MS data. Identification of major compounds was performed based on mass fragmentation patterns ( $m/z$ ) using reference compounds in MS Interpreter version 2.0. The compounds were also matched with the National Institute Standard and Technology (NIST) with MS Library V2011. Metabolites identified were filtered out based on a probability score of  $<60\%$ .

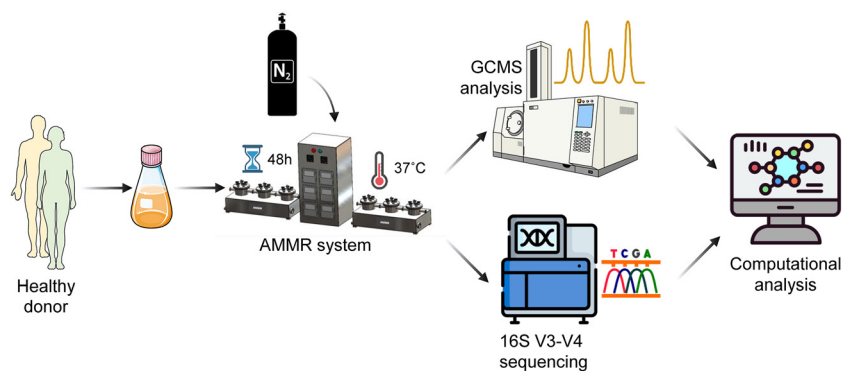


**Fig. 1** Brief experimental design of the study. Fecal samples from healthy individuals were used as inoculum for gut bacteria and treated with *L. plantarum* (probiotic) and butyrate (post-biotic) in an individual fermenter of the AMMR system. After 48 h of treatment, the samples were collected for subsequent metagenomic and metabolomic analyses.



### Metabolic pathway impact prediction

Metabolic abundance data from GC-MS analysis were used for identifying metabolic pathway impact using the Metaboanalyst V6 tool.<sup>30</sup> Kyoto Encyclopedia of Genes and Genomes (KEGG) was used as a reference library for pathway analysis and to evaluate how the identified metabolites significantly impact the general function of metabolic pathways based on the position and connectivity of metabolites within the identified and impacted pathways. The identified compounds were mapped against PubChem and KEGG identifiers.

### Metagenomic sequencing

The reaction mixtures were processed for DNA isolation and 16S rRNA amplicon sequencing. In brief, DNA isolation was carried out using a NucleoSpin Soil, Mini Kit (Cat. #740780, MACHEREY-NAGEL GmbH & Co. KG) as per the manufacturer's instructions. DNA integrity was evaluated using agarose gel electrophoresis and estimation of DNA concentration was performed using a Qubit Quant-It dsDNA HS Kit on a Qubit Fluorometer (Thermo Fisher). The V3–V4 region of the 16S rRNA genes was amplified by polymerase chain reaction with a universal forward primer and a unique barcode primer (bakt-341F: CCCTACACGACGCTCTCCGATCTG-barcode-CCTACGGGNGGCWGCAG; bakt-805R: GACTGGAGTTCCTTGGCACCCGA GAATTCCA-barcode-GACTACHVGGGTATCTAATCC). The first amplification was performed using thermal cycling conditions as follows: 94 °C for 5 min; 5 cycles of denaturation at 94 °C for 30 s, annealing at 45 °C for 20 s, and elongation at 65 °C for 30 s; 20 cycles of denaturation at 94 °C for 20 s, annealing at 55 °C for 20 s, and elongation at 72 °C for 30 s; and a final extension at 72 °C for 10 min. Illumina bridge PCR compatible primers were introduced in the second amplification as follows: 3 min of denaturation at 95 °C; 5 cycles of denaturation at 94 °C for 20 s, annealing at 55 °C for 20 s, and elongation at 72 °C for 30 s; and a final extension at 72 °C for 10 min. Amplicons were purified using AMPure XP beads, and Amplicon concentration was estimated using a Qubit 3.0 DNA Kit, and 10 ng of amplicons from each sample were sequenced using the Illumina MiSeq 2 × 300 bp platform.

### 16s rRNA sequence data analysis

Sequence data were analyzed using Quantitative Insights into Microbial Ecology (QIIME v2) by excluding primers and spacers from the sequences as previously outlined.<sup>31,32</sup> The Divisive Amplicon Denoising Algorithm 2 (DADA2) was used for trimming, denoising, merging the forward and reverse reads (paired-end), and removing chimeric sequences. OTU clustering was performed on denoised sequences using the q2-vsearch function in the QIIME2 pipeline. Forward and reverse reads were discarded if their quality was poor ( $Q < 25\%$ ). The obtained feature table was rarefied using the diversity core-metrics-phylogenetic (q2-diversity) plugin in QIIME2 at a sample depth of 12 000 to calculate microbial diversity. The diversity of microorganisms across different taxa was elucidated by using the readings from the feature table and refer-

ence taxonomic annotations from the SILVA database (version 138). Reads were obtained with 99% 16S coverage and raw taxonomy files that were trained using the Naive Bayes classifier. The trained classifier was later used using representative sequences produced by DADA2 to allocate sequences to certain taxa. Sequences constituting 0.5% of low abundance were omitted from all cases. The enrichment of microbial metabolic pathways was calculated using 16S rRNA sequences using the Phylogenetic Investigation of Communities by Reconstruction of Unobserved States (PICRUSt). Operational Taxonomic Units (OTUs) were aligned with the GreenGenes database (gg\_13\_08) using QIIME2, using a 97% similarity criterion and closed OTU selecting methodology. The abundance of OTUs was calibrated to the 16S rRNA gene copy number obtained from recognized bacterial genomes in Integrated Microbial Genomes. Anticipated functions were aligned using the Kyoto Encyclopedia of Genes and Genomes (KEGG) database.

### Statistical analysis

GraphPad V8 was used for statistical analysis of data, and quantitative data were interpreted as mean ± SEM. Metaboanalyst V6 was used for biochemical pathway enrichment utilizing a metabolite abundance list obtained from GC-MS analysis.<sup>33</sup> The enrichment ratio (ER) for the subclass was computed using observed hit/expected hit values. Holm–Bonferroni correction for the  $P$ -value and false discovery rate (FDR) was computed for each enrichment analysis entry.  $P < 0.05$  was considered significant. Linear correlation analysis between any two independent variables was done using Pearson's method. The KEGG database was used as a reference library for pathway analysis to examine functionally related metabolites and their considerable enrichment. This analysis focused on the identification of metabolites that could prevent the requirement for preselecting metabolites based on arbitrary cut-off thresholds.<sup>34</sup> The identified metabolites were cross-referred with PubChem and KEGG identifiers. Pathway analysis was performed using Fisher's exact test, and pathway impact was calculated based on the topological importance of different metabolites in a certain pathway. The metabolome and microbiome data were log-transformed and mean-centered normalized for one-factor analysis to get equal variance. The differences in microbial communities and metabolites in different treatments were analyzed using STAMP v2.1.3. For comparison,  $t$ -test (equal variance) with a  $p$ -value filter ( $>0.05$ ) was used. Extended error bar plots were made to show statistically significant values, Welch's confidence intervals, and differences in the mean proportion effect size.

## Results

### Microbiome profile

Both butyrate and *L. plantarum* differentially altered the gut microbial architecture at various taxonomic levels compared to control. At the phylum level, five considerable phyla were identified, and the gut microbiota in all three groups were pre-



dominantly composed of Firmicutes (43.61%), Bacteroidetes (35.28%), and Proteobacteria (14.31%) (Fig. 2A). Although low in abundance, Tenericutes were observed to be uniquely identified in *L. plantarum*, indicating enrichment of specific species associated with the Tenericutes phylum. Compared to the control, we found that butyrate induced a 12.0% reduction in Firmicutes and a 4.3% decrease in Bacteroidetes, accompanied by a 49.6% increase in Proteobacteria. Conversely, *L. plantarum* resulted in a 7.4% decrease in

Firmicutes, an 8.9% increase in Bacteroidetes, and a minor 3.9% rise in Proteobacteria, with negligible impacts on other phyla. As a result, the Firmicutes : Bacteroidetes (F : B) ratio demonstrated a trend of reduction due to the treatments *i.e.*, initially 1.34 in control, decreased to 1.23 ( $P = 0.35$ ) following butyrate treatment and to 1.14 ( $P = 0.12$ ) due to *L. plantarum*.

At the order level (Fig. 2B), a total of 37 orders were detected. In the control group, the gut microbiota was predominantly composed of Lactobacillales (41.55%), Bacteroidales

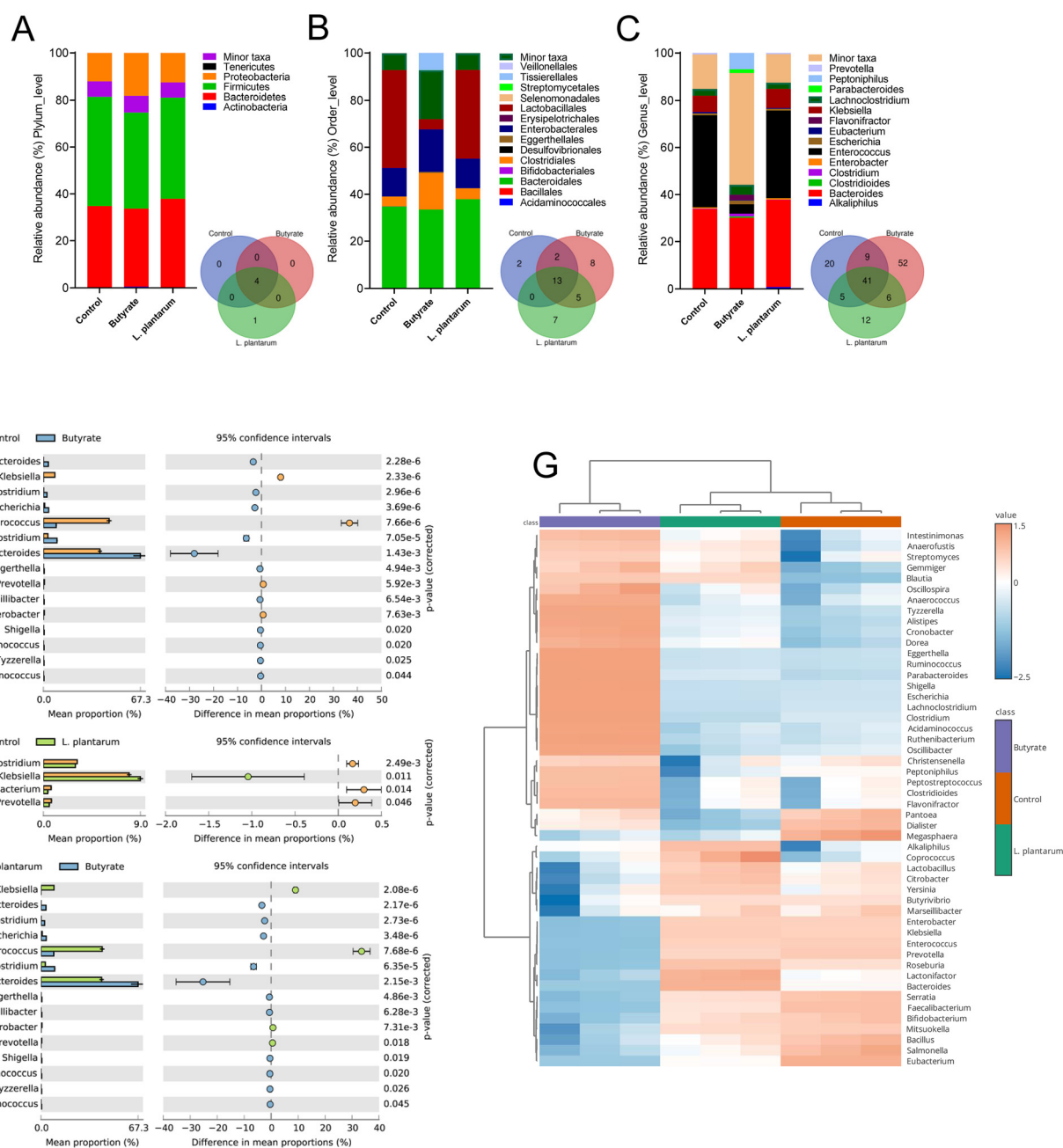


**Fig. 2** Shifts in microbiome profile in response to butyrate and *L. plantarum* treatments. (A–C) Bar plots representing relative abundance of taxa at the (A) phylum, (B) order, and (C) genus levels across the treatments. (D–F) Differential genus identification using STAMP between (D) control vs. butyrate, (E) control vs. *L. plantarum*, and (F) *L. plantarum* vs. butyrate. (G) Correlation heatmap depicting the degree of association between the identified genera and the treatments.



(34.74%), and Enterobacterales (12.12%). Following butyrate treatment, the microbial community was different, resulting in Bacteroidales (33.18%), Enterobacterales (18.07%), and Clostridiales (15.60%) emerging as the predominant groups, due to butyrate's established ability to influence gut microbial composition through anti-inflammatory short-chain fatty acid signaling. The treatment with *L. plantarum*, in contrast, reinstated a profile similar to the controls – Bacteroidales (37.82%), Lactobacillales (37.63%), and Enterobacterales (12.60%) – demonstrating its capacity for probiotic-induced community rearrangement. A direct comparison of the two interventions on the principal orders revealed that butyrate causes suppression of Lactobacillales (4.23% vs. 37.63%), moderately reduced Bacteroidales (33.18% vs. 37.82%), and increased Enterobacterales (18.07% vs. 12.60%) in relation to *L. plantarum*, underscoring the contrasting effects of a postbiotic compared to a live probiotic on essential gut taxa.

In case of genus, 145 genera were identified, of which 75, 108, and 64 absolute genera were identified in control, butyrate, and *L. plantarum* treatment groups, respectively, indicating an increased microbial diversity in the butyrate treatment group. In the control group, the three most abundant genera were found to be *Enterococcus* (39.2%), *Bacteroides* (33.7%), and *Klebsiella* (6.9%); in the butyrate treatment group, the top three genera were *Bacteroides* (30.1%), *Peptoniphilus* (6.94%) and *Lachnospirillum* (4.25%), whereas in the *L. plantarum* group the dominant genera were *Enterococcus* (37.3%), *Bacteroides* (36.9%), and *Klebsiella* (7.9%) (Fig. 2C). *Pectobacterium* (0.022%), *Flavonifractor* (2.207%), and *Micrococcus* (0.003%) were the most unique genera as identified in the control, butyrate, and *L. plantarum* groups, respectively, having the highest abundance among all the unique genera. While increasing *Parabacteroides* (0.008–1.55%) and certain butyrate-producers like *Blautia* (0.017–0.137%) and *Butyrivibrio* (0–0.005%), we observed a slight drop in *Bacteroides* after butyrate supplementation compared to control and notable decreases in classic pathobionts *Enterococcus* (39.2 → 4.0%), *Klebsiella* (6.9 → 0.01%), and *Enterobacter* (0.60 → 0.009%) were also inferred. In comparison, *L. plantarum* treatment increased *Bacteroides* and *Klebsiella* but mostly maintained high *Enterococcus* levels and had no impact on *Escherichia* and *Enterobacter*. We deduced that butyrate therapy thereby changed the gut microbiota toward lower possible pathogens and increased SCFA producers; *L. plantarum* strengthened important butyrate-producing taxa but had little effect on pathobiont suppression.

Fifteen and four differential genera were identified between control and butyrate treatment groups and control and *L. plantarum* treatment groups, respectively (Fig. 2D–F). Of note, the mean proportion of *Lachnospirillum* ( $p < 0.05$ ) was seen to be significantly higher in butyrate treatment (Fig. 2D) and significantly lower in *L. plantarum* treatment (Fig. 2E) groups when compared to the control. Butyrate treatment showed significant enrichment of *Bacteroides* (Fig. 2D and F), and *L. plantarum* treatment showed significant enrichment of

*Klebsiella* (Fig. 2E and F). The correlation heatmap of the top 50 genera with the highest abundance across the treatments showed a close association between control and *L. plantarum* treatment at the gut microbiome level. Our data indicate that butyrate treatment is positively correlated with butyrogenic and fiber-degrading genera, *i.e.*, *Intestinimonas*, *Clostridium*, *Ruminococcus*, *Shigella*, *etc.*, while some of them are negatively correlated, like *Roseburia*, *Eubacterium*, *Faecalibacterium*, *etc.* (Fig. 2G). In contrast, lactic acid-associated genera like *Lactonifactor*, *Bacteroides*, *Lactobacillus*, *etc.*, were observed to be positively correlated with *L. plantarum* treatment and negatively correlated with butyrate treatment, indicating specific enrichment of lactic acid bacteria in *L. plantarum* treatment.

### Microbial metabolic functions

Significant differences in various microbial metabolic functions were computed under butyrate and *L. plantarum* treatment, compared to the control (Fig. 3). In our study, butyrate treatment was found to redirect microbial metabolism from antibiotic and fatty acid biosynthesis to amino acid synthesis, energy metabolism, and motility (Fig. 3A). For instance, butyrate showed significantly increased processes associated with amino acid synthesis and central energy metabolism. The biosynthesis of valine, leucine, and isoleucine has shown a significant rise in addition to histidine metabolism, alanine, aspartate and glutamate metabolism, and pantothenate and CoA biosynthesis. Energy pathways such as carbon fixation *via* the citrate cycle (TCA cycle) show minor enrichments. Critical pathways for antibiotic synthesis were seen to be significantly downregulated. The production of vancomycin group antibiotics decreased considerably, as did the biosynthesis of streptomycin. The production of secondary bile acids was depleted under butyrate treatment. *L. plantarum* treatment showed limited alterations in gut microbial metabolic functions which included enrichment of pathways pertaining to ascorbate and aldarate metabolism and nucleotide excision repair, while a depletion in glycosaminoglycan degradation, histidine metabolism, and taurine and hypotaurine metabolism was noted in the *L. plantarum* group compared to control (Fig. 3B). Distinct differences in microbial function were also observed between butyrate and *L. plantarum* groups (SI Fig. S1). A total of 113 common microbial metabolic functions were predicted, out of which 1 and 7 were unique in control and butyrate treatment groups, respectively (Fig. 3C). Association heatmap coupled with sample clustering clearly indicated a close association between the control and the *L. plantarum* group, whereas butyrate resulted in altered microbial function, which was different from that of control and *L. plantarum* treatment (Fig. 3D).

### Untargeted metabolomic profile

A total of 44, 39, and 51 metabolites were identified in the control, butyrate, and *L. plantarum* groups, respectively (Fig. 4A) (SI Tables S5–S7). Although they differed in abundance, octanoic acid and capric acid were the top-abundant metabolites in all groups, followed by indole in the control





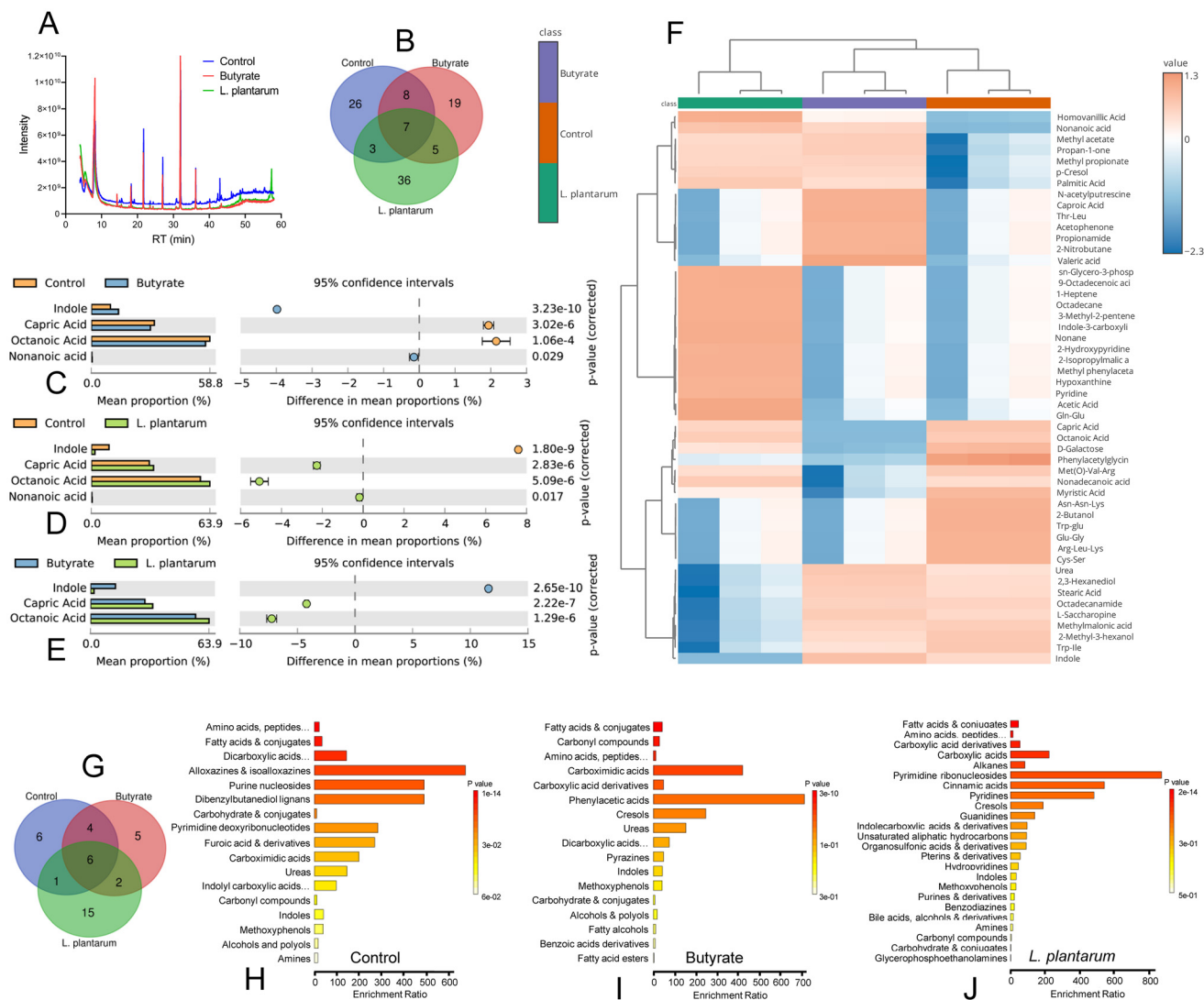


**Fig. 4** Metabolomic profiling of gut microbes under the influence of butyrate and *L. plantarum* treatments. (A) Representative GC-MS graph for all treatments with retention time (min) on the x-axis and intensity on the y-axis. (B) Venn diagram showing common metabolites identified across the treatments. (C–E) STAMP plots showing the differential abundant metabolites between (C) control vs. butyrate, (D) control vs. *L. plantarum*, and (E) butyrate vs. *L. plantarum*. (F) Correlation heatmap depicting the degree of association between identified metabolites with the treatments. (G) Venn diagram representing the metabolite class common across the treatments. (H–J) Metabolite class enrichment in (H) control, (I) butyrate, and (J) *L. plantarum* treatments. The x-axis represents the enrichment ratio value and the y-axis depicts the significance value of enrichment.

and butyrate groups, and the gln-glu peptide in the *L. plantarum* group. Seven metabolites were common among the treatments with variable abundance (Fig. 4B) (SI Table S8). These metabolites include indole, homovanillic acid, octanoic acid, capric acid, phenylacetylglucine, D-galactose, and nonanoic acid. Although the abundance of these metabolites differed across treatments, a significant difference in mean proportion was observed only in the case of indole, capric acid, nonanoic acid, and octanoic acid (Fig. 4C–E). The mean proportion of capric acid and octanoic acid ( $p < 0.05$ ) was observed to be significantly less in the butyrate treatment group (Fig. 4C), but higher in the *L. plantarum* treatment group (Fig. 4D) in comparison with the control group. The mean proportion of indole was significantly higher in the butyrate

treatment group than in the control and *L. plantarum* treatment groups (Fig. 4C and E). Unlike the correlation heatmap of genera identified and microbial metabolic functions for various treatments, the correlation heatmap of the top 50 highly abundant metabolites showed that control and butyrate treatment confer a close association in terms of metabolome data (Fig. 4F). It was seen that some of the metabolites showed similar patterns of correlation in both butyrate and *L. plantarum* treatment groups. Homovanillic acid, nonanoic acid, methyl acetate, methyl propionate, *p*-cresol, palmitic acid, etc., showed positive correlation, and phenylacetylglucine and several peptides like asn-asn-lys, trp-glu, etc., showed negative correlation with both the treatments in comparison with the control. Specifically, in *L. plantarum* treatment, 9-octa-



decanoic acid, acetic acid, indole-3-carboxylic acid, *etc.*, showed positive correlation, and urea, stearic acid, L-saccharopine, indole, *etc.*, showed negative correlation. Similarly, in butyrate treatment, *N*-acetylputrescine, caproic acid, propionamide, *etc.*, showed positive correlation, and capric acid, octanoic acid, D-galactose, myristic acid, *etc.*, showed negative correlation. The control group exhibited baseline correlations with fermentation byproducts (2,3-hexanediol) and higher aromatic metabolites, indicating unmodulated gut metabolism.

### Chemical class enrichments

Based on the identified metabolites, respective chemical class enrichments were identified. It was found that amino acid, peptides, and analogues were significantly enriched in the control, and fatty acids and conjugates in butyrate and *L. plantarum* treatment groups (Fig. 4H–J) (SI Tables S9–S11), followed by fatty acids and conjugates in the control, carbonyl compounds in the butyrate group and amino acids, peptides and analogues in the *L. plantarum* treatment group as the second significant metabolite class. In terms of the enrichment ratio, the control group showed higher enrichment of alloxazines and isalloxazines, purine nucleosides, and dibenzylbutanediol lignans (Fig. 4H). Similarly, in the butyrate group, phenylacetic acid, carboximide acids, and cresols show a high enrichment ratio (Fig. 4I); pyrimidine ribonucleosides, cinnamic acids, and pyridines were highly enriched in the *L. plantarum* group (Fig. 4J). A total of 6 metabolite classes were common across the three groups, while 6, 5, and 12 metabolite classes were inferred to be distinctly enriched in the control, butyrate, and *L. plantarum* treatment groups, respectively (Fig. 4G) (SI Table S12).

### Metabolic pathway enrichments

The identified metabolites were mapped against KEGG as a reference library for further identification of impacted pathways. The examination of metabolic pathway enrichment demonstrates unique patterns across the control, butyrate, and *L. plantarum* groups. The pathway impact analysis showed that in control, the top 3 highly impacted pathways include riboflavin metabolism (impact = 0.11), D-amino acid metabolism (impact = 0.05), and pyrimidine metabolism (impact = 0.04) (Fig. 5A) (SI Table S13). In the butyrate group, the top 3 highly impacted pathways comprise phenylalanine, tyrosine and tryptophan biosynthesis (impact = 0.04), propanoate metabolism (impact = 0.04), and pentose phosphate pathway (impact = 0.02) (Fig. 5B) (SI Table S14). The same in the *L. plantarum* group includes D-amino acid metabolism (impact = 0.17), valine, leucine and isoleucine degradation (impact = 0.15), and taurine and hypotaurine metabolism (impact = 0.14) (Fig. 5C) (SI Table S15). Six metabolic pathways were found to be common among all treatments. In contrast, butyrate showed a specific enrichment of the pentose phosphate pathway (Fig. 5D) (SI Table S16).

## Discussion

The current study was conducted to infer the differential effects of *L. plantarum* (butyrogenic probiotic)<sup>35</sup> and butyrate (postbiotic) on gut microbial population and diversity, metabolites, and associated metabolic pathways using metagenomics and metabolomics approaches. Our results indicate that *L. plantarum* and butyrate exhibit distinct yet complementary effects on gut microbes, suggesting that both live bacteria and metabolic byproducts of *L. plantarum* can confer health benefits.

The human colon, possessing the greatest microbial density among human-associated microbial communities, offers a stable anaerobic environment for many bacterial populations vital to host physiology.<sup>36</sup> Comprehending colonic biogeography and host–microbe interactions is fundamental to translational microbiome research and clinical treatment advancements, hence improving metabolic resilience. Nevertheless, research on pre-clinical and clinical colonic microbiomes exhibits significant variation, which is attributed to individual host characteristics (*e.g.*, genetics and immunological status), variations in housing and feeding, and uncontrolled fluctuations in the luminal composition.<sup>37,38</sup> Variations in transit durations, pH gradients, and mucus layers further induce compositional alterations, complicating comparison analysis among cohorts. Microbial interactions with leftover feed, bile salts, and host-secreted substances create uncontrolled chemical heterogeneity within the lumen.<sup>39</sup> These confounding variables compromise the reproducibility and translational validity of pre-clinical findings. Consequently, rigorously regulated, standardized *in vitro* or gnotobiotic models with entirely chemically specified luminal inputs are crucial to eradicate variability and facilitate reliable and reproducible mechanistic understanding. For strict gut microbial control to eliminate unnecessary variability, various *in vitro* strategies have been developed over the years to emulate the intricacies of the human gastrointestinal tract, addressing the shortcomings of fecal batch cultures and animal models.<sup>9,40,41</sup> These multicompartiment dynamic systems facilitate standardized luminal conditions and continuous or batch feeding, hence minimizing variability arising from host variables, luminal heterogeneity, and environmental variations. Thus, these *in vitro* models provide a consistent mechanistic understanding of microbial metabolism, host–microbe interactions, and the effectiveness of interventions in gut microbial research.

According to 16S rRNA gene sequencing data, *L. plantarum* reshaped the gut microbial community, irrespective of a considerable impact on the overall microbial diversity. This observation aligns with the previous pre-clinical and clinical reports that probiotics, especially belonging to the genus *Lactobacillus*, may exert health-beneficial effects without impacting the gut microbial diversity.<sup>42,43</sup> In fact, an earlier study indicated that supplementation of a single probiotic species may not be efficient enough to improve the overall diversity of the gut microbiota.<sup>44</sup> This strict nature of the gut microbiota, especially within the closed AMMR system, could be due to



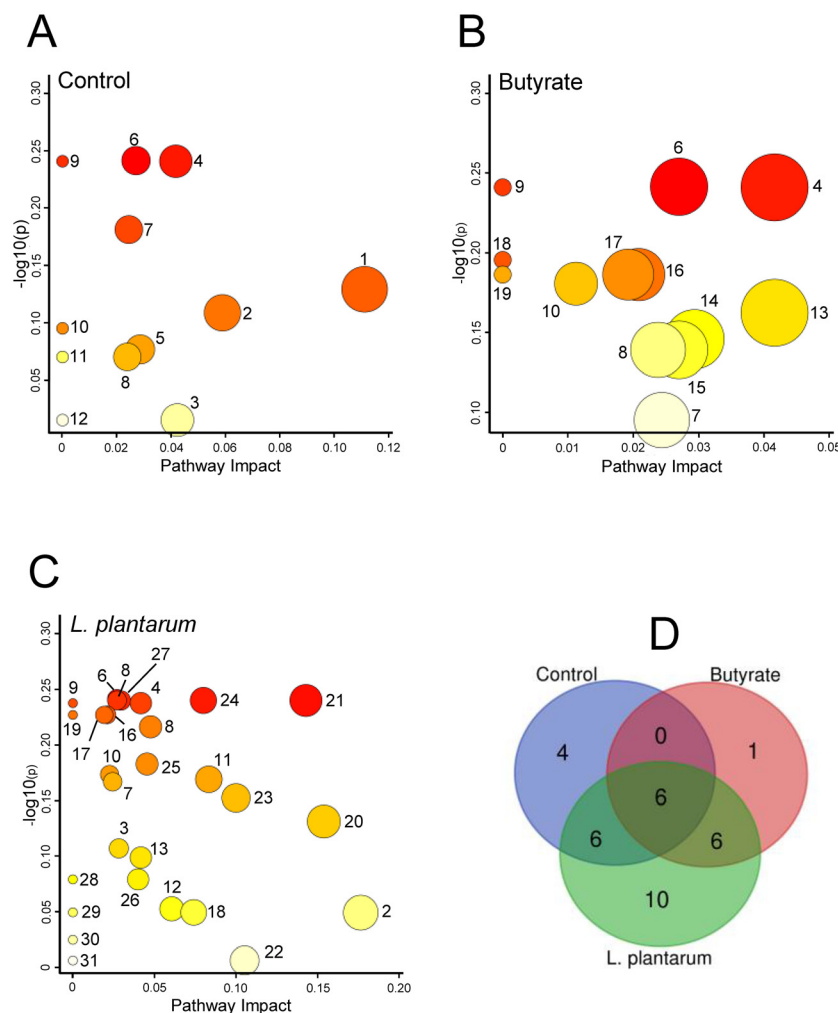


**Fig. 5** Metabolic pathway enrichment in (A) control, (B) butyrate, and (C) *L. plantarum* groups. The x-axis corresponds to the pathway impact value and the y-axis depicts the significance of the impact value. 1. Riboflavin metabolism, 2. D-amino acid metabolism, 3. pyrimidine metabolism, 4. phenylalanine, tyrosine and tryptophan biosynthesis, 5. phenylalanine metabolism, 6. lipoic acid metabolism, 7. galactose metabolism, 8. pyruvate metabolism, 9. tryptophan metabolism, 10. purine metabolism, 11. other carbon fixation pathways, 12. one carbon pool by folate, 13. propanoate metabolism, 14. pentose phosphate pathway, 15. glycolysis or gluconeogenesis, 16. fatty acid degradation, 17. fatty acid biosynthesis, 18. arginine and proline metabolism, 19. biosynthesis of unsaturated fatty acids, 20. valine, leucine and isoleucine degradation, 21. taurine and hypotaurine metabolism, 22. lysine degradation, 23. valine, leucine and isoleucine biosynthesis, 24. methane metabolism, 25. sulfur metabolism, 26. alanine, aspartate and glutamate metabolism, 27. glyoxylate and dicarboxylate metabolism, 28. selenocompound metabolism, 29. arginine biosynthesis, 30. glycine, serine and threonine metabolism, and 31. lysine biosynthesis. (D) Venn diagram representing the pathway common across the treatments.

causes such as niche occupation without displacing other community members, transient colonization and impact on the entire microbiota population, resilience nature of the core microbiome preventing displacement and colonization success by *L. plantarum*, and innate compensatory dynamics of the gut microbiota where functionally analogous spp. may bloom upon *L. plantarum*-mediated suppression of specific genera.<sup>45,46</sup>

In contrast, butyrate treatment tends to increase the gut microbial diversity (108 vs. 75) due to improved energy metabolism and cross-feeding in the gut microbial population.<sup>47</sup> Butyrate is a metabolic end-product of primary fermenters (e.g., *Faecalibacterium* and *Roseburia*), which is then used as an energy source by secondary microbial consumers.<sup>48</sup> This estab-

lishes interconnected trophic networks in which butyrate supports auxotrophic organisms that lack the ability to break down primary fibres. This cross-feeding enhances niche specialization and stabilizes the community structure, hence directly augmenting microbial diversity.<sup>49</sup> It ecologically converts butyrate into a communal resource that supports mutualistic relationships.

Differential alteration at the microbial taxonomic levels was noted in butyrate and *L. plantarum* treatment groups. The increased abundance of Proteobacteria observed following butyrate treatment remains aligned with previous reports.<sup>27</sup> Although the bloom of Proteobacteria has historically been associated with mucosal inflammation and gut-barrier dysfunction due to the presence of pyrogenic endotoxin, recent



studies indicate the diverse beneficial role of Proteobacteria that includes the production of essential vitamins,<sup>50</sup> providing colonization resistance,<sup>51</sup> and metabolic signaling.<sup>52</sup> *Tenericutes* was identified only under *L. plantarum* treatment, and this aligns with the previous report that lactic acid bacteria favor the growth of *Tenericutes*.<sup>53</sup> Our data show a decreased trend of the F : B ratio ( $P > 0.05$ ) after probiotic and postbiotic treatments. This is important since an increased F : B ratio is often associated with obesity,<sup>54,55</sup> and previous studies also showed that probiotic treatment generally decreases F : B.<sup>56</sup>

At the order level, the populations of Clostridiales, Veillonellales, and Enterobacterales were distinctly enriched due to butyrate treatment. Various members of the Clostridiales order, especially butyrate-producing species, may directly use butyrate as an energy substrate or a signaling molecule to enhance their growth and activity.<sup>57</sup> Within the AMMR system, where the nutrient availability is tightly controlled and other metabolic substrates are restricted, the direct supply of butyrate might provide a competitive advantage to these organisms, resulting in population growth. Butyrate increased the population of Veillonellales, which generally does not synthesize or utilize butyrate, but uses lactate, which is a prevalent byproduct of carbohydrate fermentation by anaerobes in the gut.<sup>58</sup> If butyrate addition increased the proliferation of primary fermenters that generate lactate, then Veillonellales would subsequently grow owing to increased substrate availability. Butyrate may also affect the community's general metabolic activity, resulting in alterations in fermentation pathways that promote lactate generation. Indeed, our data show an increased population of *Bacteroides* under butyrate treatment, which is an obligate anaerobe and follows a fermentative mode of energy production.<sup>59</sup> Interestingly, butyrate resulted in the suppression of Lactobacillales, a surprising and quite uncommon observation. Lactobacillales are well-studied lactate-producing bacteria and butyrate is typically produced due to lactate fermentation by gut microbes.<sup>60</sup> Consequently, the reduction in lactate-producing microbial orders may result from feedback inhibition caused by butyrate accumulation during feeding or from the acidic pH of the medium created by butyrate (a weak acid), as many lactate-producing species exhibit sensitivity to pH levels. At the genus level, control and *L. plantarum* groups showed similar patterns for enriched genera, but the butyrate group showed high abundance of *Peptoniphilus* and *Lachnoclostridium* in comparison with the control and *L. plantarum* groups. Both are butyrate-producing bacteria and display anti-inflammatory properties.<sup>61,62</sup> Butyrate supplementation lowers the pH of the medium, favoring the growth of butyrate-producing bacteria<sup>63</sup> and also decreases the abundance of known pathobionts (*Enterococcus*, *Klebsiella*, and *Enterobacter*). The mean proportion of *Bacteroides* and *Klebsiella* was enriched in butyrate and *L. plantarum* treatment, respectively. *Bacteroides* is a known butyrate-producing genus,<sup>64,65</sup> and evidence for increased *Klebsiella* after probiotic treatment is not present in the literature. The possible explanation for this observation could be

that probiotic treatment conferred decreased microbial diversity that normally suppresses *Klebsiella*, causing a possibility of niche expansion for it.

Metabolomics data revealed the highest enrichment of octanoic acid and capric acid in all treatments, referring to the healthy metabolome of the gut microbial population.<sup>66,67</sup> The presence of indole and *p*-cresol in high concentration in butyrate and *L. plantarum* treatment groups indicates reduced carbohydrates and increased ammonium levels, potential markers for proteolytic metabolism.<sup>68</sup> This could explain the possible reason for the identification of various peptides, like thr-leu, gln-glu, *etc.*, in both treatments. Capric and octanoic acids are the saturated fatty acids whose mean proportion was found to be higher in the *L. plantarum* treatment group in comparison with the butyrate group. Previous studies confirm that fatty acid metabolism and the saturation mechanisms of fatty acids were prominent in *L. plantarum*,<sup>69</sup> while butyrate inhibits the formation and accumulation of saturated fatty acids.<sup>70</sup> *L. plantarum* produces organic acids like lactic acid and acetic acid,<sup>71</sup> and in our results, we found a positive correlation between *L. plantarum* treatment and acetic acid. In a previous study utilizing *L. plantarum* for the treatment of high-fat-induced obesity in mice, indole-3-carboxylic acid was found to be one of the significant metabolites associated with *L. plantarum* treatment,<sup>72</sup> which confirms a positive association between indole-3-carboxylic acid and *L. plantarum* treatment as found in our study. In the case of butyrate treatment, a positive correlation was found with *N*-acetylputrescine, a polyamine, and caproic acid, a saturated fatty acid. The correlation between butyrate and polyamines is well studied, and in an experiment utilizing mouse colon cancer cells, it was found that butyrate treatment enhances the production of polyamines.<sup>73</sup> Additionally, a study by Nzeteu *et al.* explains how lactic acid and butyric acid biomass produced in a similar closed anaerobic system can help in increased production of caproic acid.<sup>74</sup>

Chemical class enrichment for each treatment revealed the significant enrichment of fatty acids and conjugates in both butyrate and *L. plantarum* treatments. In line with this, a previous study also claimed that probiotic bacteria can produce anti-inflammatory fatty acid conjugates to treat colitis.<sup>75</sup> Butyrate favors the growth of SCFA-producing bacteria,<sup>63</sup> and increased SCFA levels would lead to enrichment of fatty acids. As previously mentioned, identification of indole and *p*-cresol in butyrate and *L. plantarum* groups indicates proteolytic activities.<sup>68</sup> This justifies the identification of phenylacetic acid, an intermediate of phenylalanine metabolism, as the highest enriched chemical class and phenylalanine, tyrosine, and tryptophan biosynthesis as highly impacted pathways in butyrate treatment.<sup>76</sup> Also, in *L. plantarum* treatment, the top three impacted pathways are related to protein and amino acid metabolism. Butyrate shows specific enrichment of the pentose phosphate pathway, which aligns with the previous results demonstrating the role of butyrate in higher expression of glucose-6-phosphate dehydrogenase, a key enzyme in the pentose phosphate pathway, for nucleic acid synthesis and reactive oxygen species generation to initiate host defense.<sup>77</sup>



The gut microbial metabolic functions based on KEGG functional orthologs were computed using sequence data and further validated using the metabolomic profile. Several commonly enriched microbial pathways were identified using both approaches, while uniquely enriched pathways were identified across treatments. For instance, galactose, lipoic acid, and pyruvate metabolic pathways are universally enriched since they represent fundamental energy and redox modules in gut microorganisms.<sup>78,79</sup> Galactose catabolism generates glucose-6-phosphate for glycolysis, facilitating ATP production *via* substrate-level phosphorylation and producing NADH that propels subsequent oxidation.<sup>80</sup> Pyruvate metabolism is crucial since the pyruvate dehydrogenase complex irreversibly decarboxylates pyruvate to acetyl-CoA, connecting glycolysis to the TCA cycle for optimal ATP production by oxidative phosphorylation.<sup>81</sup> These processes produce NADH and FADH<sub>2</sub>, whose re-oxidation (*via* respiration or fermentation) maintains the NAD<sup>+</sup>/NADH equilibrium. Under anaerobic conditions, gut bacteria often convert pyruvate to lactate or ethanol to produce NAD<sup>+</sup>, hence directly associating these pathways with redox equilibrium.<sup>82</sup> Lipoic acid is an essential cofactor for pyruvate dehydrogenase and other 2-ketoacid dehydrogenases, linking carbon metabolism to electron transport; its redox-active disulfide bond also connects metabolism to oxidative stress responses.<sup>83</sup> These mechanisms together provide energy carriers (ATP), reducing equivalents, and biosynthetic precursors, constituting preserved “housekeeping” capabilities essential for microbial growth and survival. Consequently, all groups exhibit enrichment in these pathways as shown by KEGG annotations. Nevertheless, the elevated enrichment in control and *L. plantarum* groups, relative to butyrate, likely indicates active carbohydrate fermentation within those communities. *L. plantarum* and other fermentative organisms depend on efficient glycolytic and PDH/lipoate mechanisms to extract energy from carbohydrates. In contrast, the butyrate-treated group exhibited reduced enrichment, likely attributable to metabolic feedback and alterations in community dynamics. Exogenous butyrate may undergo  $\beta$ -oxidation to provide acetyl-CoA, which directly energizes the TCA cycle, potentially meeting energy requirements and inhibiting glycolysis/galactose metabolism *via* end-product feedback mechanisms.<sup>84</sup> Moreover, butyrate may promote SCFA-utilizing taxa to the detriment of sugar-fermenters, hence modifying substrate availability.<sup>85</sup> This feedback control and microbial turnover may reduce the incidence of galactose utilization and PDH-dependent genes.

In the butyrate-treated group, butyrate likely played a central role as a regulatory signal and favored energy substrate for gut microorganisms. Its presence within the closed system could be sensed as excess energy availability, resulting in feedback inhibition. In line with this, glycolysis and gluconeogenesis diminish since butyrate was the direct energy source (acetyl-CoA), hence lessening the need for glucose catabolism or anabolism.<sup>86</sup> Fatty acid biosynthesis was inhibited because butyrate, a fatty acid derivative, satisfied the requirement for additional fat.<sup>87</sup> The metabolism of lipoic acid,

essential as a cofactor in primary energy pathways such as pyruvate dehydrogenase (connecting glycolysis to the TCA cycle), subsequently diminishes when these fundamental energy-producing mechanisms become less necessary in the presence of enough butyrate.<sup>88</sup> This signifies a transition towards energy conservation and the exploitation of available butyrate.

However, in the case of the *L. plantarum* treated group, the augmentation of certain microbial metabolic pathways may be ascribed to its diverse interactions with the gut microbiota. For instance, *L. plantarum* enhances pyruvate metabolism and glyoxylate/dicarboxylate metabolism likely by acting as a trigger for glycolysis, decomposing available carbohydrates into pyruvate and phosphoenolpyruvate.<sup>89</sup> These intermediates can enter the glyoxylate shunt, circumventing decarboxylation stages in the TCA cycle, hence facilitating efficient carbon utilization for biosynthesis under low-energy conditions. Simultaneously, other carbon fixation pathways are enhanced to facilitate anaplerotic metabolic reactions, restoring oxaloacetate and succinate for the synthesis of amino acids and nucleotides.<sup>90</sup> The enhancement of valine, leucine, isoleucine, and alanine/aspartate/glutamate metabolism under *L. plantarum* can provide essential substrates for microbial growth and colonization.<sup>91</sup> Branched-chain amino acids (BCAAs) act as nitrogen donors for several metabolic pathways,<sup>92</sup> while glutamate produces glutathione.<sup>93</sup> Under *in vivo* conditions, the metabolism of arginine and proline can facilitate collagen synthesis and immune cell communication,<sup>94</sup> consistent with *L. plantarum*'s established function in improving mucosal integrity.<sup>95</sup> *L. plantarum*-induced enhancement of sulfur metabolism and taurine/hypotaurine metabolism could help alleviate oxidative stress.<sup>96</sup> The reduction of sulfur produces hydrogen sulfide, which, at healthy concentrations, can activate antioxidant mechanisms. Taurine and hypotaurine metabolism, enhanced under *L. plantarum*, can function as an effective ROS quencher. This is crucial in inflammatory environments since *L. plantarum* inhibits pro-oxidant pathogens. Collectively, *L. plantarum* functions as a metabolic coordinator, enhancing cross-feeding networks that maximize energy extraction, redox equilibrium, and structure biosynthesis, thereby explaining the extensive upregulation of several interrelated pathways.

Finally, it is to be noted that the current observations emerged out of an *in vitro* anaerobic culture system. Although the AMMR system is able to strictly control certain biochemical parameters of the human distal intestine, instruments like these are unable to capture the totality of the intricate and dynamic host–microbe interaction that is influenced by various physiological conditions like gut epithelial response, mucus layer dynamics, hormonal levels, immune cell signaling and metabolomic crosstalk. Additionally, the efficacy of probiotics and postbiotics is inherently connected to their nutritional context and food matrix. Their metabolic fate is influenced by intricate interactions within the specific functional food matrix, which includes various nutrients, fibers, and metabolites present. Consequently, outcomes observed in



a specific formulation or a simplified experimental model may not reliably predict their behaviour in a different food or within the human gut. Nevertheless, the current study provides a preliminary glimpse of how probiotics and postbiotics differentially impact the gut microbiota in a host-independent controlled environment. Furthermore, *in vivo* intervention studies are essential to validate these results.

## Conclusion

This study elucidates distinct roles of butyrate and *L. plantarum* in gut microbial activities and community composition within an *in vitro* colonic model named the AMMR system. Butyrate markedly increased total microbial diversity, likely due to improved cross-feeding, where butyrate acts as an energy substrate for secondary fermenters, promoting trophic networks and niche specialization. It inhibited both Firmicutes and Bacteroidetes while enhancing the abundance of Proteobacteria and Actinobacteria. In addition, a reduction in harmful genera (*e.g.*, *Enterococcus*, *Klebsiella*, and *Enterobacter*) was observed while selectively fostering beneficial butyrogenic taxa (*e.g.*, *Lachnospirillum* and *Blautia*). Butyrate functionally switched metabolism from antibiotic and fatty acid biosynthesis to amino acid synthesis (valine, leucine, isoleucine, and histidine), energy pathways (propanoate metabolism and pentose phosphate pathway), and motility, while reducing secondary bile acid production (suppression of inflammatory metabolic pathways). The metabolomic profile exhibited a correlation with *N*-acetylputrescine and caproic acid, indicating modifications in polyamine and fatty acid metabolism. Conversely, *L. plantarum* maintained community diversity similar to the control, exerting a small influence on the F:B ratio or prospective pathobionts (*e.g.*, *Enterococcus*). It enhanced Bacteroidetes and lactic acid bacteria, and metabolically elevated redox balance pathways (taurine/hypotaurine metabolism and sulfur metabolism) and amino acid breakdown (valine, leucine, and isoleucine), while diminishing glycosaminoglycan destruction. The metabolome exhibited a favorable association with acetic acid and indole-3-carboxylic acid, consistent with its lactic acid synthesis. In contrast to butyrate, *L. plantarum* augmented pyruvate and glyoxylate metabolism, facilitating carbon fixation and biosynthesis under low-energy conditions. Collectively, the findings of the study reveal that butyrate primarily functions as a metabolic regulator, influencing community composition and functionality *via* metabolic feedback and cross-feeding, diminishing pathogens and promoting energy and amino acid metabolism. *L. plantarum*, on the other hand, functioned as a metabolic coordinator, enhancing lactic acid bacteria and stress-response pathways without significantly modifying diversity or pathogen abundance. Therefore, the combined application of both probiotic strain and postbiotic metabolite may provide a promising basis for symbiotic formulations for enhanced gut homeostasis and alleviate gut associated metabolic disorders.

## Author contributions

NB performed the experiments, conducted the analysis and wrote the 1<sup>st</sup> draft of the manuscript along with PD; PRR edited the manuscript and supervised the project; PD supervised the project, designed the experiments, and performed the statistical analysis. All authors have read and approved the final version of the manuscript.

## Conflicts of interest

The AMMR system is the proprietary item of Fermibio Solutions Private Limited, with which Priyanka Dey & Prangya Ranjan Rout are affiliated.

## Data availability

All necessary data are included in the supplementary information (SI). Supplementary information is available. See DOI: <https://doi.org/10.1039/d5fo04976h>.

## Acknowledgements

Financial assistance from the Biotechnology Industry Research Assistance Council (BIRAC/FIT01085/BIG-20/22) is acknowledged.

## References

- 1 K. R. Pandey, S. R. Naik and B. V. Vakil, Probiotics, prebiotics and synbiotics- a review, *J. Food Sci. Technol.*, 2015, **52**, 7577–7587.
- 2 Z. Mujagic, P. D. Vos, M. V. Boekschoten, C. Govers, H.-J. H. Pieters, N. J. De Wit, P. A. Bron, A. A. Masclee and F. J. Troost, The effects of *Lactobacillus plantarum* on small intestinal barrier function and mucosal gene transcription; a randomized double-blind placebo controlled trial, *Sci. Rep.*, 2017, **7**, 40128.
- 3 N. Tewari and P. Dey, Navigating Commensal Dysbiosis: Gastrointestinal Host-Pathogen Interplay in Orchestrating Opportunistic Infections, *Microbiol. Res.*, 2024, 127832.
- 4 K. Hodgkinson, F. E. Abbar, P. Dobranowski, J. Manoogian, J. Butcher, D. Figeys, D. Mack and A. Stintzi, Butyrate's role in human health and the current progress towards its clinical application to treat gastrointestinal disease, *Clin. Nutr.*, 2023, **42**, 61–75.
- 5 J. Chen and L. Vitetta, The Role of Butyrate in Attenuating Pathobiont-Induced Hyperinflammation, *Immune Network*, 2020, **20**, e15.
- 6 N. Recharla, R. Geesala and X. Z. Shi, Gut Microbial Metabolite Butyrate and Its Therapeutic Role in Inflammatory Bowel Disease, A Literature Review, *Nutrients*, 2023, **15**, 2275.



- 7 T. Zhang, W. Zhang, C. Feng, L.-Y. Kwok, Q. He and Z. Sun, Stronger gut microbiome modulatory effects by postbiotics than probiotics in a mouse colitis model, *npj Sci. Food*, 2022, **6**, 53.
- 8 T. Van de Wiele, P. Van den Abbeele, W. Ossieur, S. Possemiers and M. Marzorati, The simulator of the human intestinal microbial ecosystem (SHIME®), in *The Impact of Food Bioactives on Health: in vitro and ex vivo models*, 2015, pp. 305–317.
- 9 Y. Qi, L. Yu, F. Tian, J. Zhao and Q. Zhai, In vitro models to study human gut-microbiota interactions: Applications, advances, and limitations, *Microbiol. Res.*, 2023, **270**, 127336.
- 10 L. Sardelli, S. Perotoni, M. Tunesi, L. Boeri, F. Fusco, P. Petrini, D. Albani and C. Giordano, Technological tools and strategies for culturing human gut microbiota in engineered in vitro models, *Biotechnol. Bioeng.*, 2021, **118**, 2886–2905.
- 11 S. Renwick, C. M. Ganobis, R. A. Elder, C. Gianetto-Hill, G. Higgins, A. V. Robinson, S. J. Vancuren, J. Wilde and E. Allen-Vercoe, Culturing human gut microbiomes in the laboratory, *Annu. Rev. Microbiol.*, 2021, **75**, 49–69.
- 12 X. Zhao, N. B. Gökgöz, Z. Xie, L. M. Jakobsen, D. S. Nielsen and H. C. Bertram, Effects of calcium supplementation on the composition and activity of in vitro simulated gut microbiome during inulin fermentation, *Food Funct.*, 2025, **16**, 2857–2869.
- 13 C. Liu, W. Jiang, F. Yang, Y. Cheng, Y. Guo, W. Yao, Y. Zhao and H. Qian, The combination of microbiome and metabolome to analyze the cross-cooperation mechanism of *Echinacea purpurea* polysaccharide with the gut microbiota in vitro and in vivo, *Food Funct.*, 2022, **13**, 10069–10082.
- 14 F. Koc, M. Sabuncu, G. G. Yavuz, G. Düven, R. M. K. Abdo, U. Bağcı, Y. Şahan, S.Ö Toğay, R. P. Ross and C. Stanton, Exploring tarhana's prebiotic potential using different flours in an in vitro fermentation model, *Food Funct.*, 2025, **16**, 4754–4771.
- 15 C. Nicco, A. Paule, P. Konturek and M. Edeas, From Donor to Patient: Collection, Preparation and Cryopreservation of Fecal Samples for Fecal Microbiota Transplantation, *Diseases*, 2020, **8**, 9.
- 16 A. L. Goodman, G. Kallstrom, J. J. Faith, A. Reyes, A. Moore, G. Dantas and J. I. Gordon, Extensive personal human gut microbiota culture collections characterized and manipulated in gnotobiotic mice, *Proc. Natl. Acad. Sci. U. S. A.*, 2011, **108**, 6252–6257.
- 17 M. Aguirre, J. Ramiro-Garcia, M. E. Koenen and K. Venema, To pool or not to pool? Impact of the use of individual and pooled fecal samples for in vitro fermentation studies, *J. Microbiol. Methods*, 2014, **107**, 1–7.
- 18 K. Newmei, S. Gorai, S. Mukherjee and P. Dey, Nrf2-dependent cytoprotective effects and depletion of gut microbial energy harvesting by chemically defined polyphenol-rich *Clerodendrum infortunatum*, *Fitoterapia*, 2025, **185**, 106730.
- 19 R. Walia, S. R. Chaudhuri and P. Dey, Reciprocal interaction between gut microbiota and aloe-emodin results in altered microbiome composition and metabolism of aloe-emodin, *Food Biosci.*, 2025, 107061.
- 20 A. Gotoh, M. Nara, Y. Sugiyama, M. Sakanaka, H. Yachi, A. Kitakata, A. Nakagawa, H. Minami, S. Okuda and T. Katoh, Use of Gifu Anaerobic Medium for culturing 32 dominant species of human gut microbes and its evaluation based on short-chain fatty acids fermentation profiles, *Biosci., Biotechnol., Biochem.*, 2017, **81**, 2009–2017.
- 21 X. Teng, T. Zhang and C. Rao, Novel probiotics adsorbing and excreting microplastics in vivo show potential gut health benefits, *Front. Microbiol.*, 2025, **15**, 1522794.
- 22 J. Armetta, S. S. Li, T. H. Vaaben, R. Vazquez-Urbe and M. O. Sommer, Metagenome-guided culturomics for the targeted enrichment of gut microbes, *Nat. Commun.*, 2025, **16**, 663.
- 23 P. Van den Abbeele, C. Grootaert, M. Marzorati, S. Possemiers, W. Verstraete, P. Gérard, S. Rabot, A. Bruneau, S. E. Aidy, M. Derrien, E. Zoetendal, M. Kleerebezem, H. Smidt and T. Van de Wiele, Microbial community development in a dynamic gut model is reproducible, colon region specific, and selective for Bacteroidetes and Clostridium cluster IX, *Appl. Environ. Microbiol.*, 2010, **76**, 5237–5246.
- 24 J. Reygnier, C. J. Condet, A. Bruneau, S. Delanaud, L. Rhazi, F. Depeint, L. Abdennebi-Najar, V. Bach, C. Mayeur and H. Khorsi-Cauet, Changes in composition and function of human intestinal microbiota exposed to chlorpyrifos in oil as assessed by the SHIME® model, *Int. J. Environ. Res. Public Health*, 2016, **13**, 1088.
- 25 G. T. Macfarlane, S. Macfarlane and G. Gibson, Validation of a three-stage compound continuous culture system for investigating the effect of retention time on the ecology and metabolism of bacteria in the human colon, *Microb. Ecol.*, 1998, **35**, 180–187.
- 26 K. P. Scott, J. C. Martin, S. H. Duncan and H. J. Flint, Prebiotic stimulation of human colonic butyrate-producing bacteria and bifidobacteria, in vitro, *FEMS Microbiol. Ecol.*, 2014, **87**, 30–40.
- 27 J. A. Jimenez, T. C. Uwiera, D. W. Abbott, R. R. E. Uwiera and G. D. Inglis, Butyrate Supplementation at High Concentrations Alters Enteric Bacterial Communities and Reduces Intestinal Inflammation in Mice Infected with *Citrobacter rodentium*, *mSphere*, 2017, **2**, e00243–17.
- 28 C. Wan, K. Wu, X. Lu, F. Fang, Y. Li, Y. Zhao, S. Li and J. Gao, Integrative analysis of the gut microbiota and metabolome for in vitro human gut fermentation modeling, *J. Agric. Food Chem.*, 2021, **69**, 15414–15424.
- 29 H. Sasaki, H. Masutomi, Y. Kobayashi, K. Toyohara, K. Imaizumi, Y. Nakayama and K. Ishihara, Evaluation of the Fermentation Characteristics of Prebiotic-Containing Granola and Short-Chain Fatty Acid Production in an In Vitro Gut Microbiota Model, *Food Sci. Nutr.*, 2025, **13**, e70252.
- 30 J. Xia, N. Psychogios, N. Young and D. S. Wishart, MetaboAnalyst: a web server for metabolomic data analysis and interpretation, *Nucleic Acids Res.*, 2009, **37**, W652–W660.



- 31 P. Dey, G. Y. Sasaki, P. Wei, J. Li, L. Wang, J. Zhu, D. McTigue, Z. Yu and R. S. Bruno, Green tea extract prevents obesity in male mice by alleviating gut dysbiosis in association with improved intestinal barrier function that limits endotoxin translocation and adipose inflammation, *J. Nutr. Biochem.*, 2019, **67**, 78–89.
- 32 X. Sun, P. Dey, R. S. Bruno and J. Zhu, EGCG and catechin relative to green tea extract differentially modulate the gut microbial metabolome and liver metabolome to prevent obesity in mice fed a high-fat diet, *J. Nutr. Biochem.*, 2022, **109**, 109094.
- 33 S. Gandhi, M. R. Saha and P. Dey, Improved antioxidant activities of spice require enrichment of distinct yet closely-related metabolic pathways, *Heliyon*, 2023, **9**, e21392.
- 34 Z. Pang, J. Chong, G. Zhou, D. A. de Lima Morais, L. Chang, M. Barrette, C. Gauthier, P. Jacques, S. Li and J. Xia, MetaboAnalyst 5.0: narrowing the gap between raw spectra and functional insights, *Nucleic Acids Res.*, 2021, **49**, W388–W396.
- 35 A. Aiello, F. Pizzolongo, L. De Luca, G. Blaiotta, M. Aponte, F. Addeo and R. Romano, Production of butyric acid by different strains of *Lactobacillus plantarum* (*Lactiplantibacillus plantarum*), *Int. Dairy J.*, 2023, **140**, 105589.
- 36 M. S. Kennedy and E. B. Chang, The microbiome: Composition and locations, *Prog. Mol. Biol. Transl. Sci.*, 2020, **176**, 1–42.
- 37 D. Laukens, B. M. Brinkman, J. Raes, M. D. Vos and P. Vandenabeele, Heterogeneity of the gut microbiome in mice: guidelines for optimizing experimental design, *FEMS Microbiol. Rev.*, 2016, **40**, 117–132.
- 38 F. Shanahan, T. S. Ghosh and P. W. O'Toole, Human microbiome variance is underestimated, *Curr. Opin. Microbiol.*, 2023, **73**, 102288.
- 39 P. Dey and S. R. Chaudhuri, The opportunistic nature of gut commensal microbiota, *Crit. Rev. Microbiol.*, 2023, **49**, 739–763.
- 40 J. Isenring, L. Bircher, A. Geirnaert and C. Lacroix, In vitro human gut microbiota fermentation models: opportunities, challenges, and pitfalls, *Microbiome Res. Rep.*, 2023, **2**, 2.
- 41 T. Shintani, D. Sasaki, Y. Matsuki and A. Kondo, In vitro human colon microbiota culture model for drug research, *Med. Drug Discovery*, 2024, **22**, 100184.
- 42 S. El Manouni El Hassani, N. K. H. de Boer, F. M. Jansen, M. A. Benninga, A. E. Budding and T. G. J. de Meij, Effect of Daily Intake of *Lactobacillus casei* on Microbial Diversity and Dynamics in a Healthy Pediatric Population, *Curr. Microbiol.*, 2019, **76**, 1020–1027.
- 43 H. Grazul, L. L. Kanda and D. Gondek, Impact of probiotic supplements on microbiome diversity following antibiotic treatment of mice, *Gut Microbes*, 2016, **7**, 101–114.
- 44 R. L. Washburn, D. Sandberg and M. A. G. Stofer, Supplementation of a single species probiotic does not affect diversity and composition of the healthy adult gastrointestinal microbiome, *Hum. Nutr. Metab.*, 2022, **28**, 200148.
- 45 G. Caballero-Flores, J. M. Pickard and G. Núñez, Microbiota-mediated colonization resistance: mechanisms and regulation, *Nat. Rev. Microbiol.*, 2023, **21**, 347–360.
- 46 P. Dey, S. R. Chaudhuri, T. Efferth and S. Pal, The intestinal 3M (microbiota, metabolism, metabolome) zeitgeist—from fundamentals to future challenges, *Free Radicals Biol. Med.*, 2021, **176**, 265–285.
- 47 H. He, H. Xu, J. Xu, H. Zhao, Q. Lin, Y. Zhou and Y. Nie, Sodium Butyrate Ameliorates Gut Microbiota Dysbiosis in Lupus-Like Mice, *Front. Nutr.*, 2020, **7**, 604283.
- 48 N. W. Smith, P. R. Shorten, E. Altermann, N. C. Roy and W. C. McNabb, The classification and evolution of bacterial cross-feeding, *Front. Ecol. Evol.*, 2019, **7**, 153.
- 49 V. R. Marcelino, C. Welsh, C. Diener, E. L. Gulliver, E. L. Rutten, R. B. Young, E. M. Giles, S. M. Gibbons, C. Greening and S. C. Forster, Disease-specific loss of microbial cross-feeding interactions in the human gut, *Nat. Commun.*, 2023, **14**, 6546.
- 50 K. Hou, Z.-X. Wu, X.-Y. Chen, J.-Q. Wang, D. Zhang, C. Xiao, D. Zhu, J. B. Koya, L. Wei and J. Li, Microbiota in health and diseases, *Signal Transduct. Target. Ther.*, 2022, **7**, 135.
- 51 L. Deng and S. Wang, Colonization resistance: the role of gut microbiota in preventing *Salmonella* invasion and infection, *Gut Microbes*, 2024, **16**, 2424914.
- 52 P. H. Bradley and K. S. Pollard, Proteobacteria explain significant functional variability in the human gut microbiome, *Microbiome*, 2017, **5**, 1–23.
- 53 S. Gupta, A. Fečkaninová, J. Lokesh, J. Koščová, M. Sørensen, J. Fernandes and V. Kiron, *Lactobacillus* Dominate in the Intestine of Atlantic Salmon Fed Dietary Probiotics, *Front. Microbiol.*, 2018, **9**, 3247.
- 54 Y. Ji, S. Park, H. Park, E. Hwang, H. Shin, B. Pot and W. H. Holzapel, Modulation of Active Gut Microbiota by *Lactobacillus rhamnosus* GG in a Diet Induced Obesity Murine Model, *Front. Microbiol.*, 2018, **9**, 710.
- 55 F. Magne, M. Gotteland, L. Gauthier, A. Zazueta, S. Pesoa, P. Navarrete and R. Balamurugan, The Firmicutes/Bacteroidetes Ratio: A Relevant Marker of Gut Dysbiosis in Obese Patients?, *Nutrients*, 2020, **12**, 1474.
- 56 Y. S. Ji, H. N. Kim, H. J. Park, J. E. Lee, S. Y. Yeo, J. S. Yang, S. Y. Park, H. S. Yoon, G. S. Cho, C. M. Franz, A. Bomba, H. K. Shin and W. H. Holzapel, Modulation of the murine microbiome with a concomitant anti-obesity effect by *Lactobacillus rhamnosus* GG and *Lactobacillus sakei* NR28, *Benef. Microbes*, 2012, **3**, 13–22.
- 57 V. Singh, G. Lee, H. Son, H. Koh, E. S. Kim, T. Unno and J. H. Shin, Butyrate producers, “The Sentinel of Gut”: Their intestinal significance with and beyond butyrate, and prospective use as microbial therapeutics, *Front. Microbiol.*, 2022, **13**, 1103836.
- 58 M. E. Salliss, J. D. Maarsingh, C. Garza, P. Łaniewski and M. M. Herbst-Kralovetz, Veillonellaceae family members uniquely alter the cervical metabolic microenvironment in a human three-dimensional epithelial model, *npj Biofilms Microbiomes*, 2021, **7**, 57.



- 59 H. M. Wexler, Bacteroides: the good, the bad, and the nitty-gritty, *Clin. Microbiol. Rev.*, 2007, **20**, 593–621.
- 60 C. Bourriaud, R. J. Robins, L. Martin, F. Kozlowski, E. Tenailleau, C. Cherbut and C. Michel, Lactate is mainly fermented to butyrate by human intestinal microfloras but inter-individual variation is evident, *J. Appl. Microbiol.*, 2005, **99**, 201–212.
- 61 S. Kim, S. H. Chun, Y. H. Cheon, M. Kim, H. O. Kim, H. Lee, S. T. Hong, S. J. Park, M. S. Park, Y. S. Suh and S. I. Lee, Peptoniphilus gorbachii alleviates collagen-induced arthritis in mice by improving intestinal homeostasis and immune regulation, *Front. Immunol.*, 2023, **14**, 1286387.
- 62 M. Vital, A. C. Howe and J. M. Tiedje, Revealing the bacterial butyrate synthesis pathways by analyzing (meta) genomic data, *mBio*, 2014, **5**, e00889.
- 63 R. B. Canani, M. D. Costanzo, L. Leone, M. Pedata, R. Meli and A. Calignano, Potential beneficial effects of butyrate in intestinal and extraintestinal diseases, *World J. Gastroenterol.*, 2011, **17**, 1519–1528.
- 64 M. A. Tufail and R. A. Schmitz, Exploring the Probiotic Potential of Bacteroides spp. Within One Health Paradigm, *Probiotics Antimicrob. Proteins*, 2025, **17**, 681–704.
- 65 P. Amiri, S. A. Hosseini, S. Ghaffari, H. Tutunchi, S. Ghaffari, E. Mosharkesh, S. Asghari and N. Roshanravan, Role of Butyrate, a Gut Microbiota Derived Metabolite, in Cardiovascular Diseases: A comprehensive narrative review, *Front. Pharmacol.*, 2021, **12**, 837509.
- 66 E. A. Franzosa, A. Sirota-Madi, J. Avila-Pacheco, N. Fornelos, H. J. Haiser, S. Reinker, T. Vatanen, A. B. Hall, H. Mallick, L. J. McIver, J. S. Sauk, R. G. Wilson, B. W. Stevens, J. M. Scott, K. Pierce, A. A. Deik, K. Bullock, F. Imhann, J. A. Porter, A. Zhernakova, J. Fu, R. K. Weersma, C. Wijmenga, C. B. Clish, H. Vlamakis, C. Huttenhower and R. J. Xavier, Gut microbiome structure and metabolic activity in inflammatory bowel disease, *Nat. Microbiol.*, 2019, **4**, 293–305.
- 67 X. Du, Q. Li, Z. Tang, L. Yan, L. Zhang, Q. Zheng, X. Zeng, G. Chen, H. Yue, J. Li, M. Zhao, Y. P. Han and X. Fu, Alterations of the Gut Microbiome and Fecal Metabolome in Colorectal Cancer: Implication of Intestinal Metabolism for Tumorigenesis, *Front. Physiol.*, 2022, **13**, 854545.
- 68 F. Candelieri, M. Simone, A. Leonardi, M. Rossi, A. Amaretti and S. Raimondi, Indole and p-cresol in feces of healthy subjects: Concentration, kinetics, and correlation with microbiome, *Front. Mol. Med.*, 2022, **2**, 959189.
- 69 S. Kishino, M. Takeuchi, S. B. Park, A. Hirata, N. Kitamura, J. Kunisawa, H. Kiyono, R. Iwamoto, Y. Isobe, M. Arita, H. Arai, K. Ueda, J. Shima, S. Takahashi, K. Yokozeki, S. Shimizu and J. Ogawa, Polyunsaturated fatty acid saturation by gut lactic acid bacteria affecting host lipid composition, *Proc. Natl. Acad. Sci. U. S. A.*, 2013, **110**, 17808–17813.
- 70 Z. Majka, B. Zapala, A. Krawczyk, K. Czamara, J. Mazurkiewicz, E. Stanek, I. Czyzyska-Cichon, M. Kepczynski, D. Salamon, T. Gosiewski and A. Kaczor, Direct oral and fiber-derived butyrate supplementation as an anti-obesity treatment via different targets, *Clin. Nutr.*, 2024, **43**, 869–880.
- 71 C. H. Hu, L. Q. Ren, Y. Zhou and B. C. Ye, Characterization of antimicrobial activity of three Lactobacillus plantarum strains isolated from Chinese traditional dairy food, *Food Sci. Nutr.*, 2019, **7**, 1997–2005.
- 72 H. Cai, Z. Wen, X. Xu, J. Wang, X. Li, K. Meng and P. Yang, Serum Metabolomics Analysis for Biomarkers of Lactobacillus plantarum FRT4 in High-Fat Diet-Induced Obese Mice, *Foods*, 2022, **11**, 184.
- 73 D. Parekh, R. Saydjari, J. Ishizuka, C. M. Townsend Jr. and J. C. Thompson, Sodium butyrate stimulates polyamine biosynthesis in colon cancer cells, *Surg. Oncol.*, 1992, **1**, 315–322.
- 74 C. O. Nzeteu, F. Coelho, A. C. Trego, F. Abram, J. Ramiro-Garcia, L. Paulo and V. O'Flaherty, Development of an enhanced chain elongation process for caproic acid production from waste-derived lactic acid and butyric acid, *J. Cleaner Prod.*, 2022, **338**, 130655.
- 75 J. Bassaganya-Riera, M. Viladomiu, M. Pedragosa, C. De Simone, A. Carbo, R. Shaykhutdinov, C. Jobin, J. C. Arthur, B. A. Corl, H. Vogel, M. Storr and R. Hontecillas, Probiotic bacteria produce conjugated linoleic acid locally in the gut that targets macrophage PPAR  $\gamma$  to suppress colitis, *PLoS One*, 2012, **7**, e31238.
- 76 N. K. Krishnamoorthy, M. Kalyan, T. A. Hediya, N. Anand, P. H. Kendaganna, G. Pendyala, S. V. Yelamanchili, J. Yang, S. B. Chidambaram, M. K. Sakharkar and A. M. Mahalakshmi, Role of the Gut Bacteria-Derived Metabolite Phenylacetylglutamine in Health and Diseases, *ACS Omega*, 2024, **9**, 3164–3172.
- 77 A. K. Rana, S. S. Kumar Saraswati, V. Anang, A. Singh, A. Singh, C. Verma and K. Natarajan, Butyrate induces oxidative burst mediated apoptosis via Glucose-6-Phosphate Dehydrogenase (G6PDH) in macrophages during mycobacterial infection, *Microbes Infect.*, 2024, **26**, 105271.
- 78 Q. Luo, N. Ding, Y. Liu, H. Zhang, Y. Fang and L. Yin, Metabolic engineering of microorganisms to produce pyruvate and derived compounds, *Molecules*, 2023, **28**, 1418.
- 79 T. Takeuchi, T. Kubota, Y. Nakanishi, H. Tsugawa, W. Suda, A. T.-J. Kwon, J. Yazaki, K. Ikeda, S. Nemoto and Y. Mochizuki, Gut microbial carbohydrate metabolism contributes to insulin resistance, *Nature*, 2023, **621**, 389–395.
- 80 A. J. Wolfe, Glycolysis for microbiome generation, *Microbiol. Spectr.*, 2015, **3**, DOI: [10.1128/microbiolspec.MBP-0014-2014](https://doi.org/10.1128/microbiolspec.MBP-0014-2014).
- 81 K. Oliphant and E. Allen-Vercoe, Macronutrient metabolism by the human gut microbiome: major fermentation by-products and their impact on host health, *Microbiome*, 2019, **7**, 1–15.
- 82 F. M. Elshaghabee, W. Bockelmann, D. Meske, M. De Vrese, H.-G. Walte, J. Schrenzenmeir and K. J. Heller, Ethanol production by selected intestinal microorganisms



- and lactic acid bacteria growing under different nutritional conditions, *Front. Microbiol.*, 2016, **7**, 47.
- 83 A. Solmonson and R. J. DeBerardinis, Lipoic acid metabolism and mitochondrial redox regulation, *J. Biol. Chem.*, 2018, **293**, 7522–7530.
- 84 D. R. Donohoe, N. Garge, X. Zhang, W. Sun, T. M. O'Connell, M. K. Bunger and S. J. Bultman, The microbiome and butyrate regulate energy metabolism and autophagy in the mammalian colon, *Cell Metab.*, 2011, **13**, 517–526.
- 85 T. van Deuren, E. E. Blaak and E. E. Canfora, Butyrate to combat obesity and obesity-associated metabolic disorders: Current status and future implications for therapeutic use, *Obes. Rev.*, 2022, **23**, e13498.
- 86 H. Liu, S. Wang, J. Wang, X. Guo, Y. Song, K. Fu, Z. Gao, D. Liu, W. He and L.-L. Yang, Energy metabolism in health and diseases, *Signal Transduct. Target. Ther.*, 2025, **10**, 69.
- 87 G. Den Besten, K. Van Eunen, A. K. Groen, K. Venema, D.-J. Reijngoud and B. M. Bakker, The role of short-chain fatty acids in the interplay between diet, gut microbiota, and host energy metabolism, *J. Lipid Res.*, 2013, **54**, 2325–2340.
- 88 M. D. Spalding and S. T. Prigge, Lipoic acid metabolism in microbial pathogens, *Microbiol. Mol. Biol. Rev.*, 2010, **74**, 200–228.
- 89 R. Chaudhry and M. Varacallo, *Biochemistry, Glycolysis*, 2018.
- 90 P. K. Arnold and L. W. S. Finley, Regulation and function of the mammalian tricarboxylic acid cycle, *J. Biol. Chem.*, 2023, **299**, 102838.
- 91 S. Starke, D. M. Harris, J. Zimmermann, S. Schuchardt, M. Oumari, D. Frank, C. Bang, P. Rosenstiel, S. Schreiber and N. Frey, Amino acid auxotrophies in human gut bacteria are linked to higher microbiome diversity and long-term stability, *ISME J.*, 2023, **17**, 2370–2380.
- 92 C. Nie, T. He, W. Zhang, G. Zhang and X. Ma, Branched Chain Amino Acids: Beyond Nutrition Metabolism, *Int. J. Mol. Sci.*, 2018, **19**, 956.
- 93 D. G. Burrin and B. Stoll, Metabolic fate and function of dietary glutamate in the gut, *Am. J. Clin. Nutr.*, 2009, **90**, 850s–856s.
- 94 V. L. Albaugh, K. Mukherjee and A. Barbul, Proline precursors and collagen synthesis: biochemical challenges of nutrient supplementation and wound healing, *J. Nutr.*, 2017, **147**, 2011–2017.
- 95 J. Wang, H. Ji, S. Wang, H. Liu, W. Zhang, D. Zhang and Y. Wang, Probiotic *Lactobacillus plantarum* promotes intestinal barrier function by strengthening the epithelium and modulating gut microbiota, *Front. Microbiol.*, 2018, **9**, 1953.
- 96 Z. Wang, Y. Ohata, Y. Watanabe, Y. Yuan, Y. Yoshii, Y. Kondo, S. Nishizono and T. Chiba, Taurine Improves Lipid Metabolism and Increases Resistance to Oxidative Stress, *J. Nutr. Sci. Vitaminol.*, 2020, **66**, 347–356.

